Hindawi
Advances in Civil Engineering
Volume 2022, Article ID 3211197, 12 pages
https://doi.org/10.1155/2022/3211197

Research Article

Investigation of Salt-Frost Heaving Rules and Mechanical Properties of Chlorite Saline Soil along the Duku Highway under Freezing-Thawing Action

Xuebang Huang,[1] **Zizhao Zhang**,[1,2] **Zezhou Guo**,[1] **Ruihua Hao**,[1] **Qianli Lv**,[1] **Tianchao Liu**,[3] **and Tiansheng Zhou**[4]

[1]*School of Geological and Mining Engineering, Xinjiang University, Urumqi, Xinjiang, China*
[2]*State Key Laboratory for Geomechanics and Deep Underground Engineering, Xinjiang University, Xuzhou, Jiangsu, China*
[3]*The First Regional Geological Survey Team of Bureau of Geology and Mineral Exploration and Development of Xinjiang Uygur Autonomous Region, Urumqi, Xinjiang, China*
[4]*Yili Kazakh Autonomous Prefecture Geological Environment Monitoring Station, Ili, Xinjiang, China*

Correspondence should be addressed to Zizhao Zhang; zhangzizhao@xju.edu.cn

Received 2 November 2021; Accepted 16 December 2021; Published 4 January 2022

Academic Editor: Bingxiang Yuan

Aiming to investigate salt-frost heaving rules and the mechanical properties of natural saline soil along the Duku Highway subjected to multiple freezing-thawing cycles, we collected natural saline soil samples from the alluvial-proluvial plain in front of the Dushanzi Mountain at the starting point of the Duku Highway. Then, we conducted mineral composition analysis tests, essential laboratory physical property measurement, large scale multiple freezing-thawing cyclic salt-frost heaving tests, shear strength tests, and unconfined compressive strength tests on the samples. According to the test results presented, the collected saline soil differed from saline soil in other regions and fell into "chlorite saline soils." As the number of freezing-thawing cycles increased, the overall salt-frost heaving capacity increased and then decreased in the freezing process but first reduced and then increased in the thawing process. Thus, the salt-frost heaving capacity was cumulative in freezing/thawing cycles. The peak salt-frost heaving capacity reached a maximum after 1 freezing-thawing cycle and then dropped drastically and fluctuated regularly. After 6 freezing-thawing cycles, the displacement deformation and time formed a new equilibrium. After 7 freezing-thawing cycles, the displacement and deformation of the soil no longer appear negative. As the number of freezing-thawing cycles increased, the cohesive force of saline soil first increased and then dropped steadily, the internal friction angle first dropped and then increased steadily, and the unconfined shear strength first increased and then decreased. These research results provided data supporting the prevention and controlling highway saline soil disasters with insightful references for the other projects in this region.

1. Introduction

With wide distribution in Xinjiang, China, saline soils have shown changing properties after repeated temperature variation over the past years, imposing adverse effects on the regular operation of engineering buildings. For example, salt-frost heaving was the main reason for the deformation and failure of road subgrades. Therefore, this study investigated salt-frost heaving rules of chlorite saline soil after multiple freezing-thawing cycles and the related changes of mechanical properties to provide adequate theoretical references for the associated failure prevention design of saline soil engineering in this region.

Previous studies revealed that sulfate and sulfite saline soil showed cumulative salt-frost heaving behaviors [1, 2]. The salt-frost heaving in saline soil under the action of freezing-thawing cycle was a volume change under the action of phase transformation of salt and crystal [3]. The

salt-frost heaving action of the soil sample at their optimum moisture content was most intense, accompanied by peak salt-frost heaving force [4]. After 4 freezing-thawing cycles, salt-frost heaving ratio began to drop after each cycle [5]. As the number of freezing-thawing cycles increased, large particle frameworks in saline soil collapsed and the finer particles rearranged [6–8].

Freezing-thawing cycles had a negative impact on soil mass [9–12]. After freezing-thawing cycles, pores among the soil particles increased and the compaction degree decreased; additionally, both pores and fractures increased proportionally, with increasing mean pore size. Simultaneously, soil structure became loose, with the framework structures in the soil showing displacement and the volume increased [13], thereby responding quickly with salt-frost heaving deformation [14–18]. Compared with the later freezing-thawing cycles, the early freezing-thawing cycle has a higher negative impact on durability and volume change. The largest volume change occurred in the first freezing-thawing cycle, and the volume change decreased with the increase of the number of freezing-thawing cycles afterwards [17, 19]. For a microscopic perspective, the freezing-thawing cycle produced crystallization pressure [18], which led to the development of cracks and the large void formed during ice melting, which increased soil permeability [20, 21]. The freezing-thawing cycles had an obvious effect, which led to the soil deformation accumulated.

The freezing temperature of the soil was an essential indicator that discerned whether the soil was frozen or not, which played a crucial role in distinguishing salt heaving from frost heaving [22]. The initial freezing temperature of soil was mainly determined by the properties of ionic solution and decreased with the increase of salt content. At the same time, it was closely related to water activity and pore size, etc. The initial freezing temperature decreased with the decrease of water activity, pore size, and unfrozen water content [23–25]. Salt heaving mainly occurred from 0°C to the initial precipitation temperature of salt crystal. The sample showed salt heaving to appear before the freezing temperature, and soil expansion included salt and frost heaving after freezing. As soil body temperature fell below −15°C, salt and frost heaving tended to become stable [26]. Salt heaving mainly occurred in the later period of saline soil with low salt content. The higher the soluble salt content, the smaller the thermal conductivity and permeability coefficient of the soil sample [27] and the greater the contribution of salt swelling to soil deformation [13, 28, 29]. At the same time, salt also migrated with water and be excluded to unfrozen water in the freezing process. With the decrease of cooling rate, the desalination rate gradually increased, and the salt crystals with cambium-like distribution in the freezing zone, influenced by the solute diffusion, form the largest distribution area of salt crystals near the freezing front [30].

Studies by some scholars showed that after multiple freezing-thawing cycles, the unconfined compressive strength, triaxial shear strength, cohesion and internal friction angle of saline soil all showed an overall loss, reflecting the damage and weakening on saline soil structure after freezing-thawing cycles [16, 17, 31]. Some scholars also showed that the cohesive force of soil first increased and then declined after multiple freezing-thawing cycles. The internal friction angle increased steadily [19, 32]. The opposite test results may be related to the type of saline soil, salt content and water content.

The Duku Highway (from now on, the Highway) crosses through the middle of the Tianshan Mountain, which began from the Dushanzi Distribution in the north and ended at Kuqa city in the south overall length of 563 km. The Highway showed incredibly profound significance in connecting southern and northern Xinjiang, shortening the traffic distance and revitalizing the economy. However, based on field investigation results, some old segments along the Highway have been partly damaged under the seasonal salt-frost heaving effect, which endangered safe traveling [33–35]. There was still a lack of systematic and wide range studies on saline soil in northwest China. Therefore, scholars mainly emphasized sulfate and sulfite saline soil in Lop Nur, ignoring chlorite saline soil on the Highway. This study focused on the saline highway segment along the Duku Highway and examined salt-frost heaving performances of saline soil to solve the above dilemma. For this work, we collected some typical natural saline soil samples for laboratory freezing-thawing cyclic tests. Conclusions were drawn for the various rules of salt-frost heaving and mechanical properties of soil samples after different cycles to provide an essential basis for preventing saline soil subgrade defects along the Highway.

2. Materials and Methods

This section is organized as follows: (1) basic physical performance parameters, (2) mineral compositions, (3) preparation of soil samples, and (4) test condition.

2.1. Basic Physical Performance Parameters. Based on the projects along the Duku Highway under construction, using a 1.2 m wooden handle flat-head shovel, some natural saline soil samples were collected from the alluvial-proluvial plain in front of the Dushanzi Mountain at the starting point of the Highway. The sampling area was in the range of 85°00′53″E–84°54′20″E and 44°14′02″N–44°10′20″N. The soil samples were sampled at a depth of 0–30 cm, with an interval of 0.5 m in one group. A total of 35 groups of soil samples were taken. Each group of soil samples weighed about 10 kg, and a total of about 350 kg of soil samples were taken. Figure 1 shows the sampling process.

According to Test Methods of Soils for Highway Engineering [36], some basic physical parameters of soil samples were measured, as shown in Table 1. Figure 2 shows the relation between dry density and moisture content. Based on the soluble salt test results in Table 2, the collected soil samples were chlorite saline soil. By combining particle sizing method and density measurement, the collected soil samples lacked particles with a size range

Figure 1: The sampling process.

Table 1: List of basic physical property parameters of saline soil.

Liquid limit, W_p (%)	25.4
Plastic limit, W_L (%)	10.1
Plastic index, I_p	15.36
Liquidity index, I_L	−0.61
Optimal moisture content, w_{opd} (%)	3.88
Maximum dry density, $\rho_{d,max}$ (g/cm^3)	1.897
Coefficient of uniformity, $C_u = d60/d10$	13.07

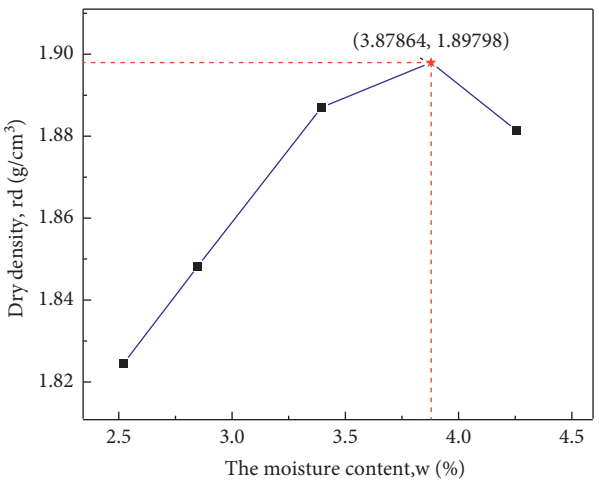

Figure 2: Curve of relation between dry density and water content.

of 0.25~0.5 mm, whereas the proportion of fine-grained particles and coarse-grained soil particles below 0.005 mm were 50.15% and 9.92%, respectively. Accordingly, we considered the collected soil as fine-grained soil. Table 3 shows the proportions of the particles with different sizes in the soil, and Figure 3 shows the measured grain composition curves.

Table 2: Sample soluble salt ion test results.

Cationic content (Mmol/kg)			Anion content (Mmol/kg)				
Ca^{2+}	Mg^{2+}	NH_4^+	$C1^-$	SO_4^{2-}	HCO_3^-	CO_3^{2-}	OH^-
0.93	0.40	0.06	2.14	1.60	3.04	0.00	0.00
Soluble salt content (%)						0.23	
CI^-/SO_4^{2-}						1.3375	
Category						Chlorous saline soil	

2.2. Mineral Compositions. X-ray diffraction technique analyzed mineral compositions of the natural saline soil samples collected from three Duku Highway locations. Table 4 shows the proportions of different mineral compositions, and Figure 4 shows the analysis results of mineral compositions. The collected natural saline soil samples were mainly composed of quartz and albite.

2.3. Preparation of Soil Samples. According to The Technical Standard of Highway Engineering [37], the compaction degree of the collected soil sample needed to be 93%. To be specific, the dry density of the compacted soil sample in the acrylic soil column instrument should be 0.93 of the maximum dry density; the moisture content of the compacted soil sample should be 3.88%, that is, the optimum moisture content; using mass control method, the dry density of the soil sample should be 1.897 g/cm^3. After obtaining moisture content, the soil sample was placed in the sealed freshness protection package for 24 hours to wet the soil thoroughly. Next, we divided the prepared soil sample into six layers, compacted using the compaction test apparatus, and placed in the soil column instrument having a size of 90 mm × 300 mm, where the fixed temperature of the sample mold was 20°C.

Table 3: Dial indicator of different particle size distribution of samples (%).

Grain size (mm)	5–20	2–5	1-2	0.5–1	0.25–0.5	0.075–0.25	0.057–0.075	0.028–0.057	0.012–0.028	0.006–0.012	0.005–0.006	<0.005
Proportion	4.91	5.72	3.21	16.35	0	19.66	10.47	15.71	9.09	4.63	0.33	9.92

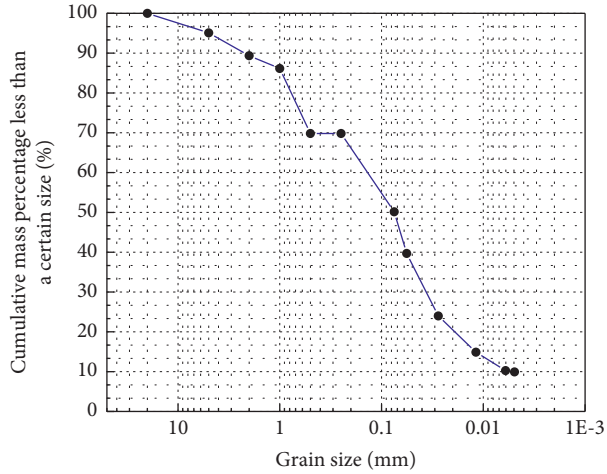

Figure 3: Grain size distribution of the soil sample.

Table 4: Mineral composition percentage of soil samples from different locations (%).

Sample	Quartz	Calcite	Chlorite	Albite	Indialite	Vaterite	Rutile	Anapaite	Muscovite
No. 1	29.7	7.2	11.5	29.1	0.4	0.2	2.2	9.9	9.8
No. 2	28.4	8.0	11.0	25.3	0.3	0.4	2.1	12.1	8.4
No. 3	36.5	9.0	8.2	32.5	0.5	0.1	2.5	10.2	7.6
The average	31.5	8.1	10.2	29.0	0.4	0.2	2.3	10.7	8.6

The preparation of triaxial test samples was similar. The soil sample was loaded into the cylindrical mold of size 39.1 mm × 80 mm. During the mold filling process, the sample was compacted in three layers. Thus, any air in the soil was reduced. After careful demolding, the compacted sample was wrapped with preservative film so as to avoid water loss. We prepared 28 triaxial soil samples in total.

The cutting-ring sample was also similarly prepared. The soil sample was loaded into the cutting ring with a size of 61.8 mm × 20 mm. During the mold filling process, the soil sample was divided into three layers and compacted. After removing air, the soil sample was wrapped by the preservative film to avoid water loss.

2.4. Test Condition. Based on air temperature data collected by the Dushanzi weather station, we analyzed the temperature data over the ten consecutive years from 2011 to 2020. As a result, the mean air temperature in summer (generally from June to August) ranged within 20~30°C, with a peak temperature of 34°C, while mean air temperature in winter (generally from December to February in the next year) ranged within −10~−18°C, with the lowest temperature of −27°C. Moreover, the low temperature fluctuated significantly in winter. Considering extreme weather, the freezing temperature and the melting temperature were −30°C and 35°C, respectively.

We first equilibrated the soil column after compaction to a temperature of 5°C for 8 hours. After temperature equilibrium, we performed the regular freezing-thawing cyclic test, during which the freezing process and the thawing process were for 12 hours. To be specific, the multifunction physical simulation platform was frozen to −30°C within half an hour and maintained at −30°C for 11.5 hours; similarly, the multifunction physical simulation platform was heated to 35°C within half an hour and held at 35°C for 11.5 hours. Accordingly, a complete freezing-thawing cycle lasted 24 hours. Figure 5 shows the temperature variation curve with temperature (Since both No. 1 and No. 2 temperature sensors, especially the No. 1 sensor, were far away from the air outlet of the box, the measured temperatures were lower than actually designed freezing and thawing temperatures). A layer of insulated cotton wrapped the soil column instrument to avoid heat exchange between the soil sample and the surrounding temperature. Thus, each soil sample underwent seven freezing-thawing cycles in total.

We used the multifunction physical simulation platform. The data acquisition system mainly consists of the DataTakerDT85G data acquisition instrument, the temperature sensor, the DeLogger data acquisition software, the displacement sensor, and the computer. The constantan thermocouple was used as the temperature sensor, with a measuring range of −50~50°C, whose temperature probe

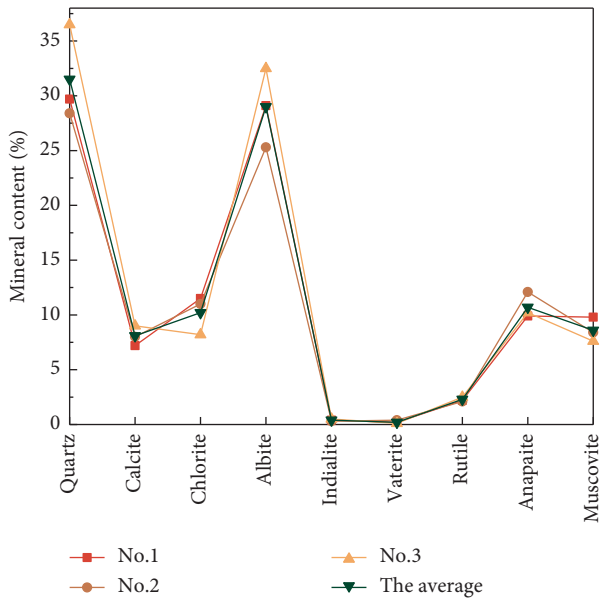

Figure 4: Mineral composition analysis diagram.

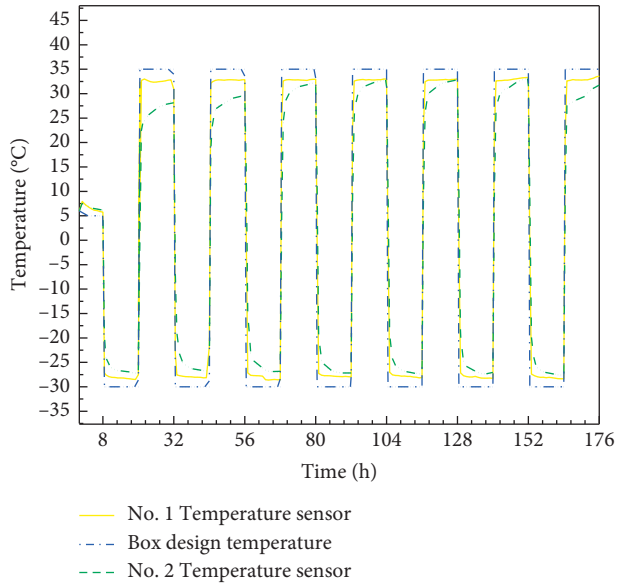

Figure 5: Box temperature during freezing-thawing cycle.

comprises two materials (copper and constantan). Before the use, the temperature sensor was cemented with AB glue to be sealed and waterproofed. The D050 displacement sensor was used, and according to the parameter settings listed in Table 5, the temperature-induced effect was automatically compensated. At the start of a test, temperature and displacement sensors were calibrated before being initialized.

The ZJ-type strain controlled direct shear instrument was adopted for the direct shear testing. According to the Direct Shear Test in Standard for the Soil Test Methods for Highway Engineering [36], the direct shear test was performed on cutting ring saline soil samples after different numbers of freezing-thawing cycles, during which vertical pressure was 50 kPa, 100 kPa, 150 kPa, and 200 kPa, respectively. The variation rules for shear strength and the related parameters of saline soil samples after different freezing-thawing cycles were then analyzed based on the direst shear test data.

The YW-2 strain controlled unconfined pressure gangue was adopted for the unconfined compressive strength test. According to the Unconfined Compressive Strength Test in Standard for the Soil Test Methods for Highway Engineering [36], the unconfined compressive test was performed on triaxial soil samples after different numbers freezing-thawing cycles to conclude the variation rules of unconfined compressive strength in freezing-thawing cycles. Figure 6 shows the drawing of the test device.

3. Results and Analysis

3.1. Salt-Frost Heaving Rules. Taking the natural chlorinated saline soil of the Duku Highway as the research object, through indoor large size soil column simulation test, the salt-frost heaving law of saline soil under different freezing-thawing cycles was obtained. See Figures 7–11 and Table 6 for details.

According to the variation of the displacement deformation with time after different numbers of freezing-thawing cycles (Figure 7), the deformation was divisible into four stages.

(1) The first stage is fast cooling and the subsequent lag (in the first two hours). At this stage, before an hour, the displacement deformations of soil samples after 1, 2, and 3 freezing-thawing cycles increased at a decreasing rate; the displacement deformations of soil samples after 4 and 5 freezing-thawing cycles tended to be stable; the displacement deformations of soil samples after 6 and 7 freezing-thawing cycles dropped at an increasing rate. After an hour, the displacement deformations of soil samples after the 2nd, then 3rd, then 4th, then 5th, then 6th, and the 7th freezing-thawing cycles decreased at an increasing rate, but the deformation after the first cycle increased.

(2) The second stage is constant freezing (from the 2nd hour to the 12th hour). The displacement deformations of soil samples after 1 and 2 freezing-thawing cycles tended to be stable. However, the displacement deformation of soil samples after 3, 6, and 7 cycles first dropped and then increased, while the deformations of soil samples after 4 and 5 cycles decreased.

(3) The third stage is rapid heating and the subsequent lag (from the 12th hour to the 14th hour). At the first half of the set (from the 12th hour to the 13th hour), the deformations of soil samples after 4 freezing-thawing cycles increased, while those after 1, 2, 3, 5, 6, and 7 cycles decreased. At the second half of the stage (from the 13th hour to the 14th hour), the deformations of soil samples after 2 freezing-thawing cycles dropped, while those of soil samples after 1, 3, 5, 6, and 7 cycles increased.

Table 5: Displacement sensor parameters.

Product model	Range (mm)	Accuracy of measurement (mm)	Connection mode	Service temperature range
D050	50	0.01	Half-bridge	−35°C~70°C

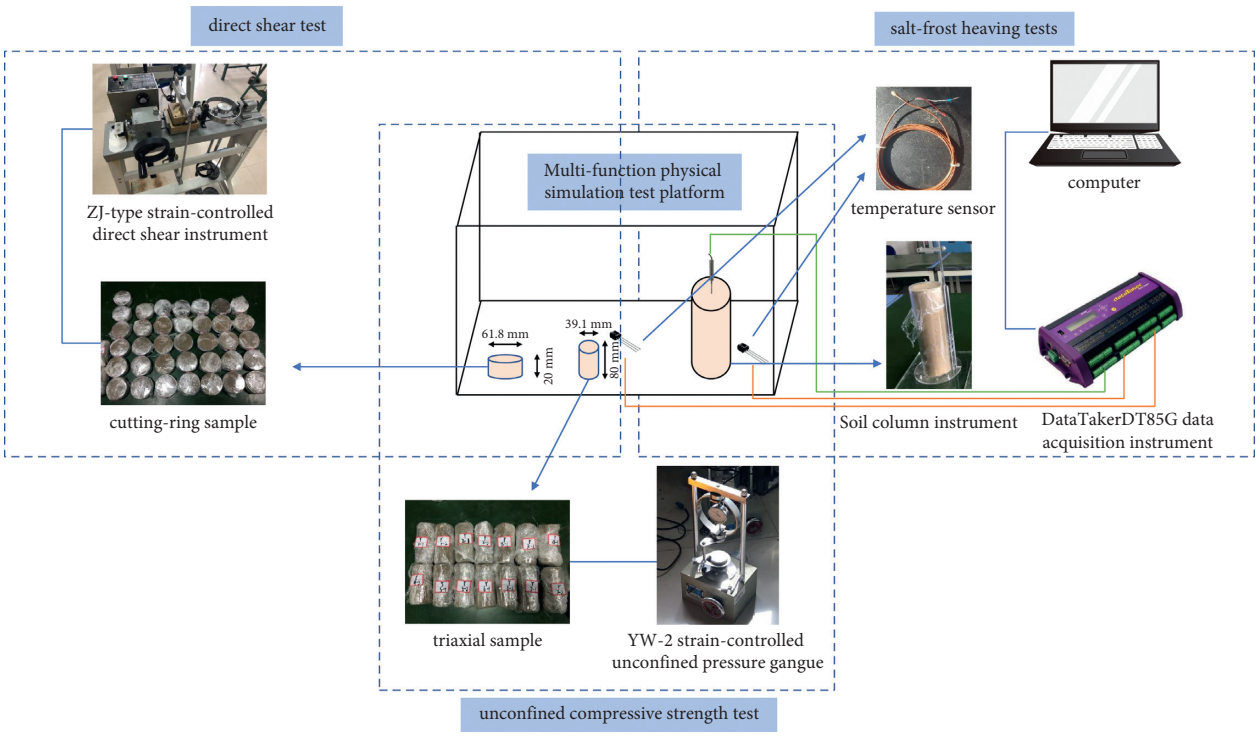

Figure 6: Test device drawing.

(4) The fourth stage is continuous thawing phase (from the 14th hour to the 24th hour). At this stage, the deformations of soil samples after 1~7 freezing-thawing cycles all increased.

At rapid freezing and the subsequent lag stage, the box temperature became frozen to −30°C within half an hour. During the rapid cooling and its hysteresis stage, although the temperature drops sharply, it took some time for the temperature to go from the periphery of the soil to the inside of the soil. Therefore, the salt-frost heave occurred 1 h after the rapid cooling and the salt-frost heaving phenomenon. Obviously, the displacement and deformation of the soil sample increased drastically after 1 freezing-thawing cycle. The salt frost heaving destroyed the soil structure with the increasing number of freezing-thawing cycles; that is, giant skeletons in soil were decomposed into small frames, supplemented with supplementing the original pore structures. Meanwhile, after freezing-thawing cycles, the proportion of pores and pore diameter increased, accompanied by loosening of soil structure. Overall, thaw collapse of soil can offset or exceed the produced salt-frost heaving capacity. Therefore, after 2 and 3 freezing-thawing cycles, the displacement deformations increased at decreasing rate. After 4 and 5 freezing-thawing cycles, the displacement deformations tended to be stable, while those after 6 and 7 cycles increased. Figure 8 shows the temporal variation curves of the displacement deformation of chlorite saline soil (the enlarged drawing in the first 2 hours), from which we concluded that salt-frost heaving was cumulative. After an hour, the temperature outside the soil column was transferred to the inside, accompanied by increasing thaw collapse volume. After 1 freezing-thawing cycle, soil's salt-frost heaving capacity still exceeded thaw collapse induced by soil structure decomposition, leading to the overall steady increase of displacement deformation. As the number of freezing-thawing cycles increased, the soil structure's destruction was more evident; soil's thaw collapse far exceeded soil's salt-frost heaving capacity, and, accordingly, soil deformation dropped rapidly at a decreasing rate.

At a constant freezing stage, the freezing temperature of the box remained constant. Therefore, when the outside temperature fully matched the inside of the soil column, salt-frost heaving capacity replaced the soil collapse induced by soil structure decomposition after a freezing-thawing cycle. Therefore, the displacement deformation of the soil sample tended to be stable. After 4 and 5 freezing-thawing cycles, soil's salt-frost heaving capacity dropped steadily, while those after 3, 6, and 7 cycles first decreased and then increased because of the damaged soil structure to a specific limit with the increasing freezing-thawing cycles. Therefore, soil's salt-frost heaving capacity increased steadily. In the meantime, soil contraction no longer appeared after seven

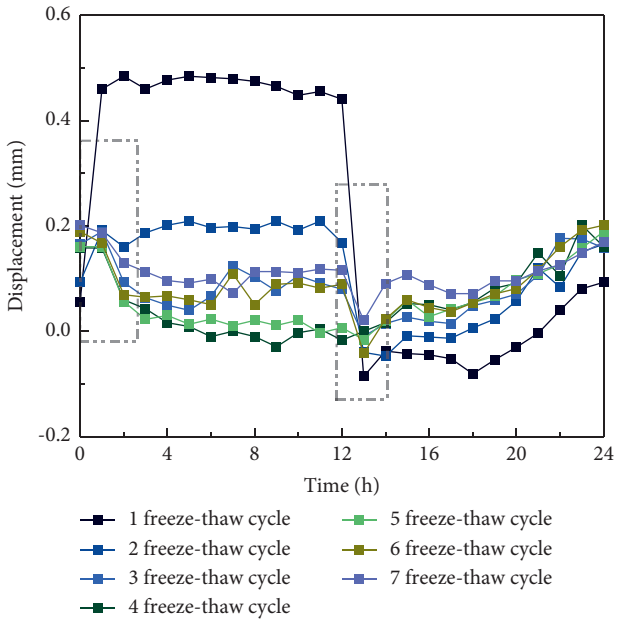

Figure 7: Curve of displacement and deformation.

freezing-thawing cycles; that is, the displacement deformation of soil was always positive, which confirmed the cumulative property of salt-frost heaving. Nevertheless, it occurred, particularly in the first 3 freezing-thawing cycles. Soil samples after 3 freezing-thawing cycles showed different displacement deformation tendencies from those after 4 and 5 cycles but were similar to those after 6 and 7 cycles in displacement deformation.

At rapid heating and the subsequent lag stage, frost heaving that initially appeared at low temperature began to thaw with fast temperature rise. Figure 9 shows the temporal variation curves of the displacement deformation of chlorite saline soil (the enlarged drawing in 12–14 hours). At low temperature, soil frost heaving exceeded salt heaving, and the thawing capacity induced frost heaving exceeded salt heaving capacity, leading to a drastic decline in soil displacement deformation. Soil samples after different numbers of freezing-thawing cycles expect 4 cycles followed the above rules. Since the thawing capacity induced by frost heaving of soil sample after 4 freezing-thawing cycles was smaller than the increment of salt heaving capacity, and the displacement deformation after 4 freezing-thawing cycles still increased with the increasing temperature.

At the constant thawing stage, the box temperature was constant. As a result, NaCl crystals in the soil dissolved in water. As a result, part of the soil collapsed because of lack of support, while the other soil underwent no collapse under various internal forces. Therefore, soil overall collapse capacity was smaller than the increment of salt heaving capacity. Meanwhile, particle vibration amplitude increased with increasing temperature for the soil sample with low salinity and moisture content. As a result, soil heaving capacity exceeded the thawing capacity induced by salt-frost heaving, leading to increased displacement deformation.

Conclusively, soil deformation after 1~7 freezing-thawing cycles increased steadily on account of cumulative salt-frost heaving behaviors.

As shown in Figure 10, the deformation induced by salt-frost heaving of soil sample after 1 freezing-thawing cycle reached the peak. Next, as the number of freezing-thaw cycles increased, soil deformation showed similar variation tendencies with temperature, which arrived at a new equilibrium after 6 cycles. The displacement deformation of soil showed a "w"-shaped variation with time. Additionally, the temporal variation curve included a small tail.

As shown in Figure 11, soil's peak salt-frost heaving capacity after 1 freezing-thawing cycle fluctuated regularly since the 2nd cycle, which tended to be stable after 6 freezing-thawing cycles. Therefore, it was predictable that the salt-frost heaving capacity will increase stably. In the initial freezing-thawing cycle test, the moisture content of the soil column was optimal, so the peak salt frost heave was reached after 1 freezing-thawing cycle, but as the temperature rose repeatedly, the moisture content in the soil column decreased. Therefore, after the number of freezing-thawing cycles in the later period, the salt-frost heave amount of the soil did not change much, showing regular fluctuations. However, as the number of freezing-thawing cycles further increased, the salt-frost heaving was promoted. Therefore, the salt-frost heaving of saline soil increased after 7 freezing-thawing cycles, and it was predicted that the salt-frost heaving amount of saline soil will increase as the number of freezing-thawing cycles further increase.

3.2. Shear Stress Curves of Soil Samples after Different Numbers of Freezing-Thawing Cycles. Taking saline soil ring knife samples as the research object, through the indoor direct shear test, the relationship between the shear strength of the soil sample and the vertical pressure under different freezing and thawing cycles was obtained. See Figures 12 and 13 for details.

As shown in Figure 12, soil's shear strength reached the maximum after 3 freezing-thawing cycles and dropped to the minimum after 2 cycles. After 3 cycles, the shear strength of the soil sample was most significant, followed by the value after 6, 7, 4, 1, and 5 cycles, while the shear strength of the sample after two cycles was the lowest. As shown in Figure 13, under a vertical pressure of 50 kPa, shear strength of saline soil showed no apparent relation between the number of freezing-thawing cycles; as the vertical stress increased to over 100 kPa, soil's shear strength first increased and then decreased with the increasing number of cycles. Thus, it was predictable that the shear strength dropped steadily until the maximum shear strength with increased freezing-thawing cycles.

3.3. Effect of the Number of Freezing-Thawing Cycles on Shear Strength Parameter. Through indoor tests, direct shear tests were performed on the saline soil ring cutter samples after different freezing-thawing cycles, in order to obtain the change law of the shear strength parameters (including cohesion and internal friction angle) of the soil samples under different freezing-thawing cycles. See Figure 14 for details.

Table 6: The variation trend of displacement with time under different freezing-thawing cycles.

Time	1 freezing-thawing cycle	2 freezing-thawing cycle	3 freezing-thawing cycle	4 freezing-thawing cycle	5 freezing-thawing cycle	6 freezing-thawing cycle	7 freezing-thawing cycle
0-1 h	Increase	Increase	Increase	Smooth	Smooth	Reduce	Reduce
1-2 h	Increase	Reduce	Reduce	Reduce	Reduce	Reduce	Reduce
2–12 h	Smooth	Smooth	First decrease and then increase	Reduce	Reduce	First decrease and then increase	First decrease and then increase
12-13 h	Reduce	Reduce	Reduce	Increase	Reduce	Reduce	Reduce

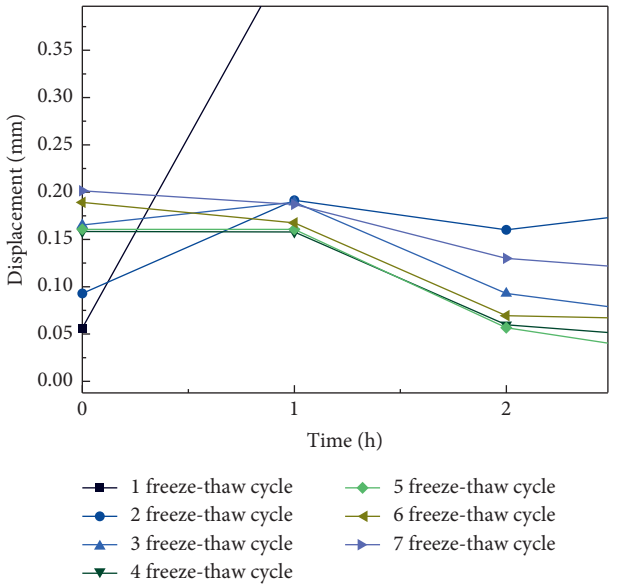

Figure 8: Curve of displacement and deformation (0–2 h local amplification).

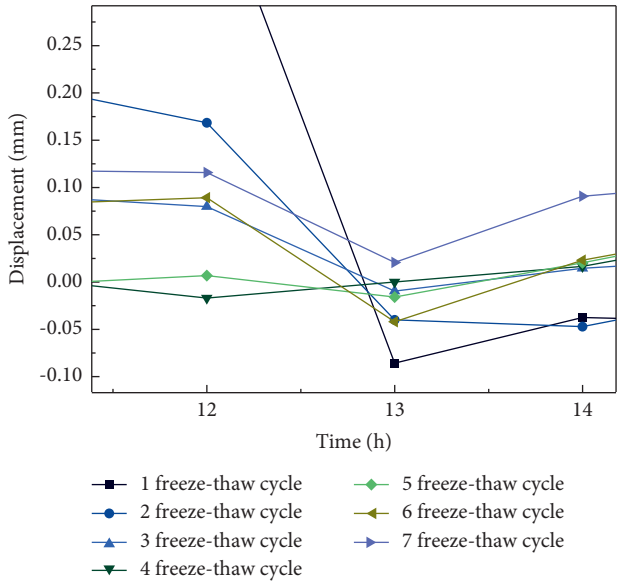

Figure 9: Curve of displacement and deformation (local magnification in 12–14 h).

The shear strength parameter of saline soil resulted from the combined effects from salinity, moisture content, the number of freezing-thawing cycles, external temperature,

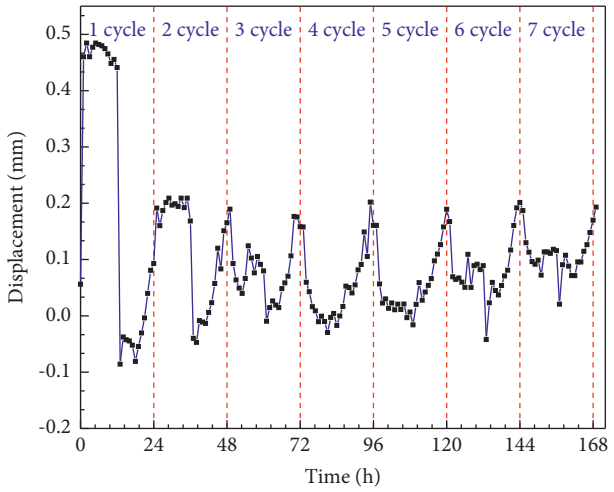

Figure 10: Salt-frost heaving process and duration curve of chlorite saline soil.

soil structure, the compaction degree, soil particle shape and grading, and the mineral compositions [38].

As shown in Figure 14, as the number of freezing-thawing cycles increased, soil's cohesive force first increased and decreased steadily. The cohesion of the soil sample reaches the maximum after 2 freezing-thawing cycles, and the maximum value reaches 5.09 kN/m^2. The value after 3 cycles decreased rapidly, while the value after 4 cycles began to increase again. Overall, the cohesive force of soil dropped with the increasing number of freezing-thawing cycles. After 2 freezing-thawing cycles, the cohesive force of the soil sample was more significant than that after 1 cycle. After a few freezing-thawing cycles, the freezing of water in pores increased the concentration of soluble salt in water because of freezing-thawing cyclic action, leading to the precipitation of soluble salt crystals and the increase in structural strength. Therefore, the cohesive force of saline soil increased to a certain degree. The cohesive force of soil samples after 3~7 freezing-thawing cycles overall decreased. The increased freezing-thawing cycles destroyed the soil's compact structure, and the soil strength decreased. Moreover, the reduction of soil strength was cumulative. All these can account for the first increase and then steady decrease of cohesive soil force.

Soil's internal friction angle first decreased and increased steadily with the increased freezing-thawing cycles. The internal friction angle of the soil sample reached the minimum after 2 freezing-thawing cycles, and the minimum

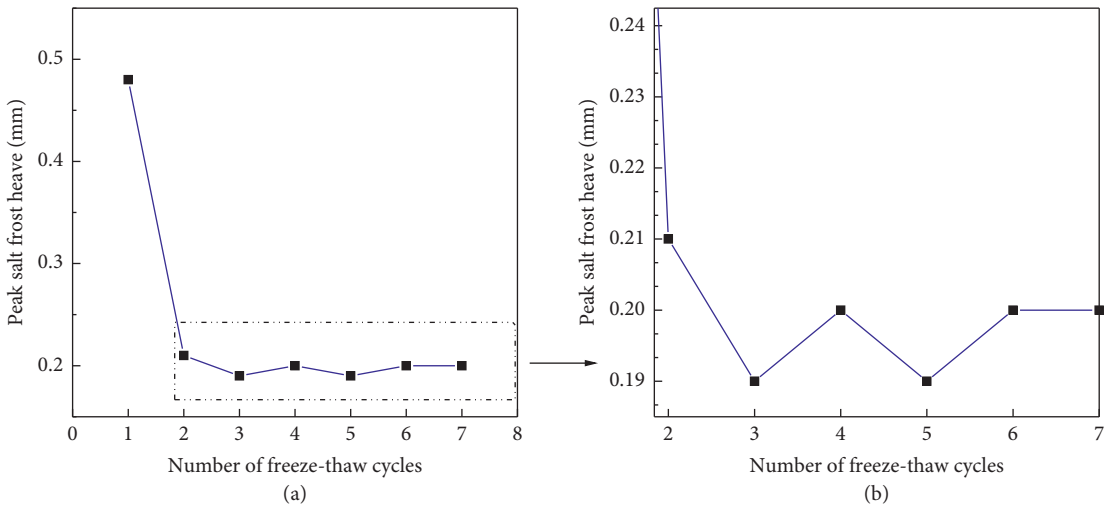

Figure 11: Relationship between peak salt-frost heave and number of freezing-thawing cycles.

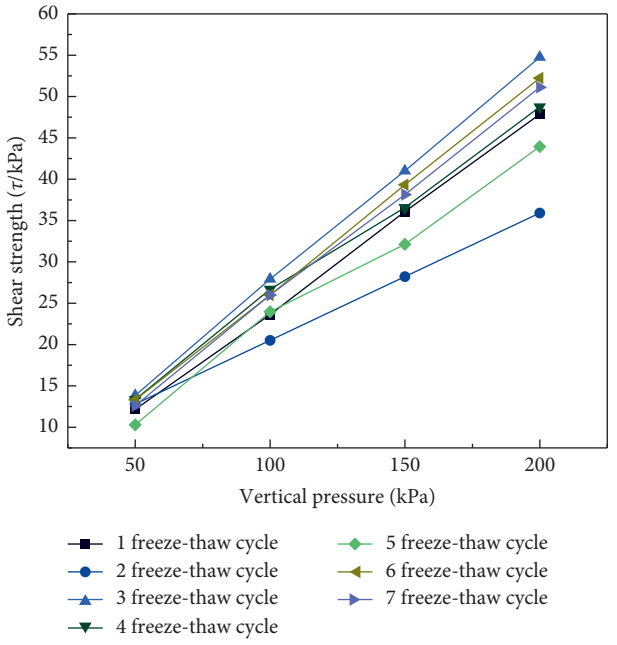

Figure 12: Relationship between shear strength and vertical pressure under different freezing-thawing cycles.

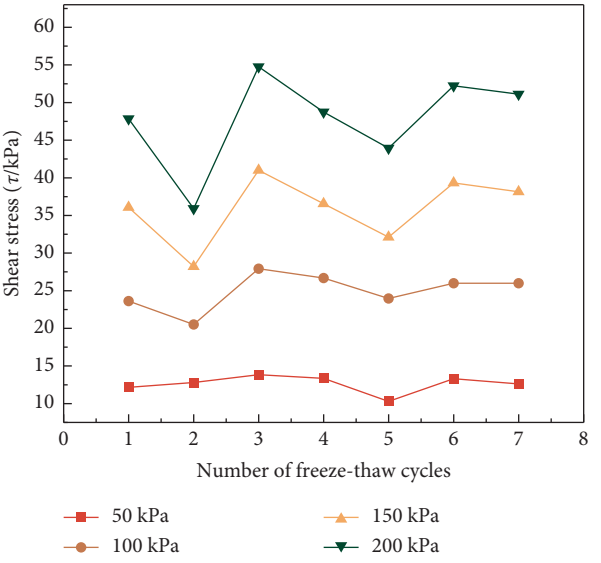

Figure 13: Relationship between shear strength and freezing-thawing cycles under different pressures.

reached 8.76°, while after 3 cycles, it reached the maximum, and the maximum reached 15.20°. The following two reasons explained this. On the one hand, water and salt migrated towards the top of the soil sample in freezing-thawing cycles [20, 39, 40], which caused uneven water and salt distribution in the sample. On the other hand, solid particle water film decreased in thickness and lubrication effect; meanwhile, large particles in soil were decomposed into smaller particles in freezing-thawing cycles, leading to increased contact areas among particles and therefore the sliding friction force.

Additionally, as the number of freezing-thawing cycles increased, the degree of soil compaction decreased steadily, and the porosity increased gradually, leading to the decline in dislocation and rotation of particles around the shear surface and the weakening in directional rearrangement of particles. Accordingly, the occlusive friction dropped steadily. Since the increase of the sliding friction force was lower than the decline in the occlusive friction in the early stage, the growth of the sliding friction exceeded the decrease in the occlusive friction. Therefore, the variation curves' turning points occurred with the 2nd and 3rd freezing-thawing cycles.

3.4. Unconfined Compressive Strength Test. Taking the triaxial samples of saline soil after different freezing and thawing cycles as the research object, the unconfined compressive strength test of the soil samples under different freezing and thawing cycles was obtained through the unconfined compressive strength test. See Figure 15 for details.

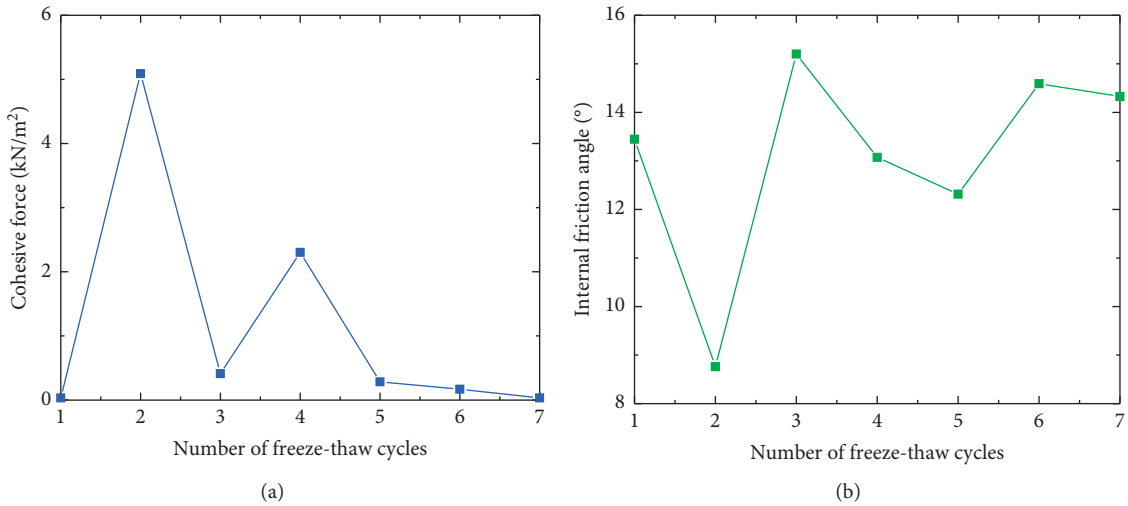

Figure 14: Relationship between shear strength parameter and number of freezing-thawing cycles: (a) cohesive force and (b) internal friction angle.

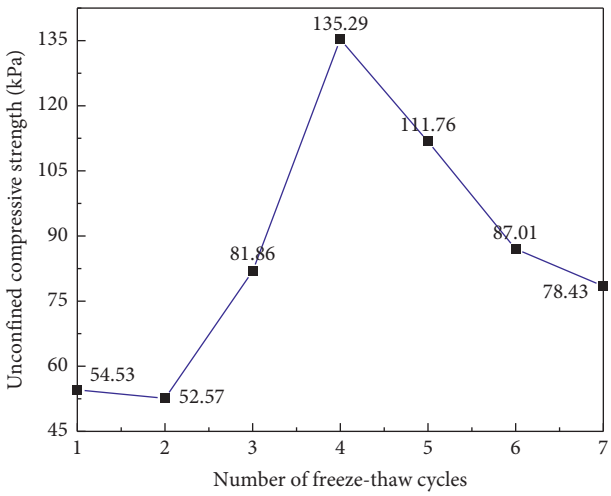

Figure 15: Relationship between unconfined compressive strength and freezing-thawing cycles.

As shown in Figure 15, the relation curve between unconfined compressive strength and the number of freezing-thawing cycles first increased and then decreased steadily. The unconfined compressive strength of the soil sample after 4 freezing-thawing cycles reached the maximum, and the maximum value reached 135.29 kPa. It was predictable that the unconfined compressive strength decreased to the minimum with the increasing number of freezing-thawing cycles.

With the increase in the number of freezing-thawing cycles, the large-particle framework of the soil structure was destroyed into small-particle frameworks, which reduced the strength of the soil. However, due to the low salt content of the research object, the results of previous experiments showed that in the freezing and thawing process, the decrease of the salt content increases the strength of the soil [41]. The interaction between the freezing-thawing cycle and the salt content made the unconfined compressive strength of the soil reach the maximum after 4 freezing-thawing cycles. Subsequently, as the number of freezing-thawing cycles increased, the strength of the soil began to decrease.

4. Discussion

This study focused on natural saline soil on the Duku Highway, Xinjiang, and performed a large size salt-frost heaving test, direct shear test, and unconfined compressive strength test after multiple freezing-thawing cycles for investigating the effects of freezing-thawing cycles on displacement deformation and mechanical properties. According to the observed test results, chlorite saline soil samples collected from the Duku Highway showed particular salt-frost heaving and mechanical properties under cyclic freezing-thawing action. In the salt-frost heaving test, the displacement deformation first increased and then decreased at the freezing stage, which first dropped and then increased at the thawing stage. Thus, the deformation characteristics of the soil sample at the thawing stage are different from previous research results. Furthermore, they considered the present soil sample's low salinity and moisture content, the increase of salt-frost heaving capacity at the thawing stage was because of enhanced soil particle activity at high temperature. Therefore, soil heaving capacity finally exceeded the thawing capacity in salt-frost heaving. Nevertheless, the cumulative salt-frost heaving behaviors are consistent with previous studies, suggesting that sulfate, sulfite, and chlorite saline soil samples were cumulative in the salt-frost heaving process.

As the number of freezing-thawing cycles increased, cohesive force first increased and then dropped steadily. The cohesive force of the soil sample after 2 freezing-thawing cycles reached the maximum. The internal friction angle first decreased and then increased steadily. After two cycles, the internal friction angle dropped to the minimum while the value after 3 cycles reached the maximum. After 2 freezing-thawing cycles, the shear strength of the soil sample dropped

to the minimum, while the value after 3 cycles increased to the max. The cohesion negatively correlates with the shear strength, and the internal friction angle is positively correlated with the shear strength, indicating the more significant effect of internal friction angle on the shear strength than that of cohesive force. It was previously suggested that the shear strength of the soil sample with higher salinity dropped more significantly and early [7]. This study focused on chlorite saline soil with low salinity, whose shear strength first increased to the maximum after 3 freezing-thawing cycles and then dropped steadily. As the number of freezing-thawing cycles increased, the unconfined compressive strength increased and dropped significantly, unlike previous studies. Since both failure stress and failure strain of saline soil decreased with the increasing number of freezing-thawing cycles, soil strength with low salinity increased in the freezing-thawing process. The unconfined compressive strength of soil increased in the first 4 freezing-thawing cycles, which reached the maximum after the 4th cycle; subsequently, the increased cycles destroyed the soil structure, and the unconfined compressive strength began to drop.

One shortcoming of this study lies in the insufficient freezing-thawing cycles. Consequently, the variation after the seventh freezing-thawing cycle followed previous research findings. There were no microscopic tests performed in this study. Instead, the microstructural rules were based on past theoretical analysis.

5. Conclusions

(1) The salt-frost heaving amount of chlorite saline soil, like sulfate and sulfite saline soil, also exhibited an additive property during freezing-thawing cycles. As the number of freezing-thawing cycles increased, the salt-frost heaving amount of chlorinated saline soil first increased and then decreased during the freezing stage and first reduced and then increased during the thawing stage. In addition, it reached the maximum peak salt-frost heave amount after 1 freezing-thawing cycle and did not contract after 7 cycles.

(2) With the increased in the number of freezing-thawing cycles, the cohesive force of chlorite saline soil first increased and then dropped steadily, which reached the maximum after 2 freezing-thawing cycles; the internal friction angle first decreased and then increased steadily, which reached the maximum after 3 freezing-thawing cycles; its shear strength reached the maximum after 3 freezing-thawing cycles. It is predicted that the influence of the internal friction angle on the shear strength of the soil under the action of freezing-thawing cycles is greater than the cohesive force.

(3) As the number of freezing-thawing cycles increased, the unconfined compressive strength of chlorite saline soil first increased and then dropped, which reached the maximum after 4 freezing-thawing cycles.

Data Availability

The data used to support the findings of this study are included within the article.

Conflicts of Interest

The authors declare that there are no conflicts of interest.

Acknowledgments

The authors gratefully acknowledge financial support for this research from the Open Foundation of State, Key Laboratory for Geomechanics and Deep Underground Engineering (SKLDUEK2028), and the Special Program for Key Research and Development Tasks of Xinjiang Uygur Autonomous Region (2021B03004).

References

[1] C. P. Chu, B. Li, and Z. J. Hou, "Salt expansion accumulation of sulphate salty soil under freezing and thawing cycles," *Journal of Glaciology and Geocryology*, vol. 20, pp. 108–111, 1998, in Chinese.

[2] W. X. Bao, X. H. Yang, and Y. L. Xie, "Research on salt expansion of representative crude saline soil under freezing and thawing cycles," *Chinese Journal of Geotechnical Engineering*, vol. 28, pp. 1991–1995, 2006, in Chinese.

[3] T. Wen, S. Ying, and F. Zhou, "Calculation of salt-frost heave of sulfate saline soil due to long-term freeze-thaw cycles," *Sci. Cold Arid Reg.*vol. 12, pp. 284–294, 2020.

[4] J. Ci, Y. F. Zhang, and S. S. Na, "Law of salt expansion of Lop Nors nature saline soil under condition of freeze -thaw cycle," *J. Water Resour. Water Eng.*vol. 7, pp. 194–197, 2016, in Chinese.

[5] L. Pan, Y. F. Zhang, J. Z. Cheng et al., "Research on salt -frost expansion rules of sulfurous saline soil during each freeze -thaw cycle," *J. Water Resour. Water Eng.*, vol. 29, pp. 220–224+231, 2018, in Chinese.

[6] S. S. Zhang, Y. L. Xie, X. H. Yang et al., "Research on microstructure of crude coarse grain saline soil under freezing and thawing cycles," *Rock and Soil Mechanics*, vol. 31, pp. 123–127, 2010, in Chinese.

[7] W. Zhang, J. Ma, and L. Tang, "Experimental study on shear strength characteristics of sulfate saline soil in Ningxia region under long-term freeze-thaw cycles," *Cold Regions Science and Technology*, vol. 160, pp. 48–57, 2019.

[8] C. J. Liu, Z. Zhang, L. T. Zhang et al., "Influence of freeze-thaw cycles on shear strength parameters of natural saline soil," *J. Water Resour. Archit Eng.*vol. 17, no. 1, pp. 73–76, 2019, in Chinese.

[9] B. Yang, D. Li, S. Yuan, and L. Jin, "Role of biochar from corn straw in influencing crack propagation and evaporation in sodic soils," *Catena*, vol. 204, Article ID 105457, 2021.

[10] B. Yang, J. Liu, X. Zhao, and S. Zheng, "Evaporation and cracked soda soil improved by fly ash from recycled materials," *Land Degradation & Development*, vol. 32, no. 9, pp. 2823–2832, 2021.

[11] B. Yang, K. Xu, and Z. Zhang, "Mitigating evaporation and desiccation cracks in soil with the sustainable material biochar," *Soil Science Society of America Journal*, vol. 84, no. 2, pp. 461–471, 2020.

[12] B. B. Yang, S. Yuan, Y. Liang, and J. Liu, "Investigation of overburden failure characteristics due to combined mining: case study, Henan Province, China," *Environmental Earth Sciences*, vol. 80, 2021.

[13] J. Zhang, Y. Lai, J. Li, and Y. Zhao, "Study on the influence of hydro-thermal-salt-mechanical interaction in saturated frozen sulfate saline soil based on crystallization kinetics," *International Journal of Heat and Mass Transfer*, vol. 146, Article ID 118868, 2020.

[14] J. L. Qi, A. V. Pieter, and G. D. Cheng, "A review of the influence of freeze-thaw cycles on soil geotechnical properties," *Permafrost and Periglacial Processes*, vol. 17, no. 3, 2006.

[15] D. Chang and J. K. Liu, "Review of the influence of freeze-thaw cycles on the physical and mechanical properties of soil," *Sci. Cold Arid Reg.*vol. 5, pp. 457–460, 2013.

[16] Z. Cheng, G. Cui, Z. Yang et al., "Improvement of the salinized soil properties of fly ash by freeze-thaw cycles: an impact test study," *Sustainable Times*, vol. 13, pp. 1–23, 2021.

[17] J. Wang, Q. Wang, S. Lin et al., "Relationship between the shear strength and microscopic pore parameters of saline soil with different freeze-thaw cycles and salinities," *Symmetry Plus*, vol. 12, pp. 1–19, 2020.

[18] D. Wu, Y. Yang, X. Zhou, and Y. Wang, "An experimental study of heat and mass transfer in deformable sulfate saline soil during freezing," *Heat and Mass Transfer*, vol. 55, no. 6, pp. 1809–1817, 2019.

[19] Y. Sun, Y. F. Zhang, D. M. Zhou et al., "Research on strength variation laws of natural saline-soil in Lop Nur under freeze-thaw cycles. Water resour," *Architect and Engineer*, vol. 12, pp. 121–124, 2014, in Chinese.

[20] X. Zhang, Q. Wang, G. Wang et al., "A study on the coupled model of hydrothermal-salt for saturated freezing salinized soil," *Mathematical Problems in Engineering*, vol. 2017, 2017.

[21] E. J. Chamberlain and A. J. Gow, "Effect of freezing and thawing on the permeability and structure of soils," *Developments in Geotechnical Engineering*, vol. 26, pp. 73–92, 1979.

[22] Z. Xiao, Y. Lai, and M. Zhang, "Study on the freezing temperature of saline soil," *Acta Geotechnica*, vol. 13, no. 1, pp. 195–205, 2018.

[23] X. Wan, Y. Lai, and C. Wang, "Experimental study on the freezing temperatures of saline silty soils," *Permafrost and Periglacial Processes*, vol. 26, no. 2, pp. 175–187, 2015.

[24] H. Bing and W. Ma, "Laboratory investigation of the freezing point of saline soil," *Cold Regions Science and Technology*, vol. 67, no. 1-2, pp. 79–88, 2011.

[25] X. Wan and Z. Yang, "Pore water freezing characteristic in saline soils based on pore size distribution," *Cold Regions Science and Technology*, vol. 173, Article ID 103030, 2020.

[26] J. C. Wang, J. S. Li, and C. M. Wang, "Study on single cycle salt and frost heaving of sulfate (sulfurous) saline soil," *Journal of Jilin University (Earth Science Edition)*, vol. 03, pp. 410–416, 2006, in Chinese.

[27] S. Zhang, J. Zhang, Y. Gui, W. Chen, and Z. Dai, "Deformation properties of coarse-grained sulfate saline soil under the freeze-thaw-precipitation cycle," *Cold Regions Science and Technology*, vol. 177, Article ID 103121, 2020.

[28] H. Bing and P. He, "Experimental investigations on the influence of cyclical freezing and thawing on physical and mechanical properties of saline soil," *Environmental Earth Sciences*, vol. 64, no. 2, pp. 431–436, 2011.

[29] J. Zhang, Y. Lai, Y. Zhao, and S. Li, "Study on the mechanism of crystallization deformation of sulfate saline soil during the unidirectional freezing process," *Permafrost and Periglacial Processes*, vol. 32, no. 1, pp. 102–118, 2021.

[30] P. Viklander, "Permeability and volume changes in till due to cyclic freeze/thaw," *Canadian Geotechnical Journal*, vol. 35, no. 3, pp. 471–477, 1998.

[31] T. Kamei, A. Ahmed, and T. Shibi, "Effect of freeze-thaw cycles on durability and strength of very soft clay soil stabilised with recycled Bassanite," *Cold Regions Science and Technology*, vol. 82, pp. 124–129, 2012.

[32] S. Maimaitiyusupu, S. C. Tao, and Alimu, "Experimental study on deformation and strength characteristics of chlorinated saline soil under freeze thaw cyeles," *Science Technology and Engineering*, vol. 19, pp. 267–272, 2019, in Chinese.

[33] Y. Wu, J. Cui, J. Huang, W. Zhang, N. Yoshimoto, and L. Wen, "Correlation of critical state strength properties with particle shape and surface fractal dimension of clinker ash," *International Journal of Geomechanics*, vol. 21, no. 6, Article ID 04021071, 2021.

[34] B. Bai, Q. Nie, Y. Zhang, X. Wang, and W. Hu, "Cotransport of heavy metals and SiO2 particles at different temperatures by seepage," *Journal of Hydrology*, vol. 597, Article ID 125771, 2021.

[35] B. Bai, G. Yang, T. Li, and G. Yang, "A thermodynamic constitutive model with temperature effect based on particle rearrangement for geomaterials," *Mechanics of Materials*, vol. 139, Article ID 103180, 2019.

[36] Research Institute of Highway Ministry of Transport, *Test Methods of Soils for Highway Engineering. JTG 3430-2020*, Ministry of Transport of the People's Republic of China, Beijing, China, 2020.

[37] Ministry of Communications Highway Division and China Association for Engineering Construction Standardization, *Technical Standard of Highway Engineering. JTG B01-2003*, Ministry of Transport of the People's Republic of China, Beijing, China, 2003.

[38] Y. M. Long, "Influence factor study of remolded cohesive soil's c φ values," Edited by J. Cent, Ed., MA Thesis in Chinese, South University, Georgia, USA, 2012.

[39] X. Zhang, Q. Wang, T. Yu et al., "Numerical study on the multifield mathematical coupled model of hydraulic-thermal-salt-mechanical in saturated freezing saline soil," *International Journal of Geomechanics*, vol. 18, 2018.

[40] S. Wang, J. Ding, J. Xu et al., "Shear strength behavior of coarse-grained saline soils after freeze-thaw," *KSCE J. Civ. Eng.*vol. 23, 2019.

[41] B. Hui and H. Ping, "Experimental investigations on the influence of cyclical freezing and thawing on physical and mechanical properties of saline soil," *Environmental Earth Sciences*, vol. 64, pp. 431–436, 2011.